Toxicology International
DOI: 10.18311/ti/2026/v33i3/55034
INFORMATICS JOURNALS
eISSN: 0976-5131 | Vol 33(3), 2026 | pp. 501-512

Production of Soluble Recombinant Human PH20 Hyaluronidase in CHO Cell Line

Chirag G. Patel[1], Rajabrata Bhuyan[1], Ekta Tyagi[1], Akanksha Kotiya[1], Pracheta Janmeda[1], Prabhakar[2*], and Anand Prakash[1*]

[1]Department of Bioscience and Biotechnology, Banasthali Vidyapith, Banasthali – 304022, Rajasthan, India; anandprakash@banasthali.in; prabhakar@sarsuagenterprises.com

[2]Sarsuag Enterprises, Bengaluru – 560100, Karnataka, India

Abstract

Hyaluronidase plays an important role in the temporary degradation of Hyaluronan/ Hyaluronic Acid (HA), a major barrier to bulk fluid movement in the subcutaneous space, thereby enhancing the absorption and bioavailability of co-administered drugs. In this study, a patented soluble recombinant human PH20 (rHuPH20) was used. The patented PH20 sequence has a truncated site at the carboxyl region responsible for membrane anchoring, enabling secretory expression. In our study, structural prediction using AlphaFold and molecular dynamics simulations confirmed the stability of the rHuPH20 enzyme. The gene was cloned into a eukaryotic expression vector (pcDNA3.1(+)) and stably transfected into a CHO-K1 cell line for protein expression. The secreted rHuPH20 was purified through affinity purification. Furthermore, Purified hyaluronidase (rHuPH20) exhibited measurable enzymatic activity of around 100000 IU/ML. These results demonstrated the successful production, purification, and functional activity of soluble rHuPH20. The purpose of this study is to understand the thermostability, cloning, production and efficacy of patented rHuPH20, thereby establishing a benchmark for novel hyaluronidase.

Major Findings : (i) Engineered PH20 structure. (ii) Clone E10 highest expression. (iii) High-purity PH20 protein.

Keywords: Expression System, Drug Delivery, Hyaluronidase, Subcutaneous, Therapeutic Enzyme

1. Introduction

Hyaluronidase is an enzyme that catalyses the depolymerisation of hyaluronic acid (HA), a high molecular weight glycosaminoglycan and an essential component of the extracellular matrix[1]. Hyaluronan is made up of D-glucuronic acid disaccharide units and N-acetyl-D-glucosamine, contributing to tissue hydration, viscoelasticity, and structural organisation. Due to its high water-binding capacity, HA forms a hydrated matrix that supports cell migration, proliferation, and signalling processes. The biological function of HA depends on its molecular weight, with high-molecular-weight HA generally associated with tissue homeostasis. In contrast, lower molecular weight fragments are involved in inflammation and cellular responses[2,3].

Hyaluronidases are a family of glycosidases, distributed across the animal kingdom and are known to modulate extracellular matrix homeostasis. Based on the classification by Meyer, enzymes are categorised into three types - hyaluronoglucosaminidases, mammalian and venom-derived enzymes that hydrolyze β-1,4-glycosidic bonds in hyaluronan to produce N-acetylglucosamine-terminated oligosaccharides, hyaluronoglucosidases, such as leech enzymes, which cleave β-1,3-glycosidic bonds to yield glucuronic acid-terminated oligosaccharides, and hyaluronate lyases, microbial enzymes that degrade β-1,4 linkages via an elimination mechanism, generating unsaturated disaccharides[4-6]. They are also functionally classified by their optimal activity: acid-active hyaluronidase (pH 3.0-4.0, e.g., human liver, serum, and certain animal toxins) and neutral-active hyaluronidase (pH 5.0-8.0, the majority)[7].

Article Received on: 23.02.2026 **Revised on:** 10.05.2026 **Accepted on:** 03.06.2026

**Author for correspondence*

In humans, five hyaluronidase isozymes (HYAL1, HYAL2, HYAL3, HYAL4, and PH20/SPAM1) are widely expressed, each with distinct tissue distribution, enzymatic properties, and physiological roles[8,9]. HYAL1 is the major lysosomal enzyme active in plasma and somatic tissues, whereas HYAL2 functions at the cell surface, initiating hyaluronan degradation, and HYAL3/4 have comparatively less defined roles. Among these, human PH20 (also known as SPAM1) is unique due to its Glycosylphosphatidylinositol (GPI)-anchored localisation on sperm and its ability to degrade hyaluronan under both neutral and acidic pH conditions. PH20 is well-suited for therapeutic applications because of its dual pH activity, effective hydrolysis of β 1-4 glycosidic bonds, and low immunogenicity[10]. Particularly for large molecules, the degradation of HA by rHuPH20 has important therapeutic applications (Biotechnology Therapeutics). By increasing the penetration of co-administered medications, hyaluronidase (rHuPH20) facilitates faster and more reliable absorption through the subcutaneous route of administration[11].

The regulatory approval of HERCEPTIN® SC and HYQVIA®, which co-formulate monoclonal antibodies with rHuPH20, by the Food and Drug Administration (FDA) in 2014 and the European Medicines Agency (EMA) in 2013, respectively, marked a major clinical milestone[12]. This innovation offers several benefits: reduced infusion time, increased patient convenience, and comparable efficacy and safety profiles to IV routes. As of 2025, eight hyaluronidase co-formulated products have received global regulatory approval, reaching from oncology to immunodeficiency indications. These include HERCEPTIN HYLECTA™ (trastuzumab + hyaluronidase) for HER2-positive breast cancer, RITUXAN HYCELA® (rituximab + hyaluronidase) for B-cell malignancies, PHESGO® (trastuzumab + pertuzumab + hyaluronidase) for HER2-positive breast cancer, DARZALEX FASPRO® (daratumumab + hyaluronidase) for multiple myeloma, VYVGART® HYTRULO (efgartigimod alfa + hyaluronidase) for generalised myasthenia gravis and CIDP, OCREVUS ZUNOVO™ (ocrelizumab + hyaluronidase) for multiple sclerosis, TECENTRIQ HYBREZA™ (atezolizumab + hyaluronidase) for solid tumours, and OPDIVO QVANTIG™ (nivolumab + hyaluronidase) for a range of cancers. These formulations enable rapid subcutaneous delivery of large-volume biologics, reducing infusion times to minutes and improving patient convenience while maintaining therapeutic efficacy[13-16].

The wild-type HuPH20 is anchored on the cell membrane and is poorly secreted, which requires molecular engineering for efficient recombinant production (EP4194551). This study emphasises cloning and recombinant expression of a secretory hyaluronidase.

In the previous study, Halozyme reported a proprietary sequence of recombinant hyaluronidase having secreted hyaluronidase with improved stability and efficacy[17]. The recombinant human PH20 (rHuPH20) hyaluronidase from the Halozyme patent was selected for this study. The sequence was cloned into the mammalian expression vector pcDNA3.1(+) followed by stable transfection in the CHO-K1 cell line. For downstream processing and analytical assays, polyclonal antibodies against recombinant hyaluronidase were generated in rabbits. The expressed protein was subsequently purified via bead-based affinity column purification. Therefore, secretory rHuPH20 was cloned and expressed using stable transfection, providing a basis for its functional and structural studies. Hyaluronidase has broad clinical applications, ranging from dermatology and oncology to its recent use as a co-administration agent that enhances the subcutaneous delivery of large molecules. To date, only a few companies have reported and patented recombinant human PH20 (rHuPH20). Although animal-derived hyaluronidase has been widely used, its higher immunogenicity has manifested a significant risk in human applications. The recent approval of clinical trials highlights the importance of rHuPH20, and the development of new variants may provide future therapeutic options[13].

2. Materials and Methods

The wild-type hyaluronidase is membrane-bound and poorly secreted. Hence, a truncated sequence from the Halozyme patent has been used for cloning in a mammalian expression vector[18].

2.1 Protein Structure Modelling

The three-dimensional structure of the engineered hyaluronidase PH-20 (rHuPH20) enzyme was predicted using the AlphaFold server[19]. The best generated model was retrieved in PDB format for subsequent molecular dynamics simulations.

2.2 Molecular Dynamics Simulation

GROMACS 2024 was used to evaluate the structural solidity of the engineered hyaluronidase PH-20.

CHARMM36 energy field was used to generate protein structure files[20,21]. The system was solvated with the Transferable Intermolecular Potential with 3 Points (TIP3P) water model and neutralised by adding appropriate concentrations of sodium (Na^+) and chloride (Cl) ions in a cubic box with periodic boundary conditions to keep a minimum distance of 1nm from the protein surface. Energy minimisation was performed using the steepest descent algorithm for 50,000 steps to achieve optimal system energetics.

The systems were equilibrated in two steps after energy minimisation: first in the NVT ensemble for 200ps and then in the NPT ensemble for 200 ps. The temperature was controlled at 300K using a modified Berendsen thermostat, while the pressure was maintained at 1 atm by using the Berendsen barostat. Long-term electrostatic interactions were treated using the particle mesh Ewald method in combination with a cut-off distance of 1nm for Van der Waals interactions. For apoprotein, Molecular Dynamics (MD) production simulations lasting for 100ns each were run. Simulations utilised a 2fs integration time step, with coordinate snapshots saved every 10ps for subsequent analysis.

2.3 Structural Stability Analysis

To evaluate the conformational stability and dynamic behaviour of the enzyme structures, several analyses were performed on the MD trajectories. Root Mean Square Deviation (RMSD) values were calculated for protein backbone atoms (C, Cα, N), while Root Mean Square Fluctuation (RMSF) was computed for Cα atoms, and the radius of gyration (Rg) was calculated to assess the compactness and folding behaviour of the enzyme structure throughout the simulation period. All trajectory analyses were performed using GROMACS built-in analysis tools, and results were visualised using XMGRACE software (https://plasma-gate.weizmann.ac.il/pub/grace/).

2.4 Mammalian Cell Transfection Using Polyethylenimine (PEI)

Mammalian cell stable transfection was performed using Polyethylenimine (PEI) following an optimised protocol[22,23]. Briefly, high-quality, endotoxin-free plasmid DNA encoding the protein of interest was prepared in *E. coli* and quantified spectrophotometrically. One day before transfection, CHO-K1cells were seeded in 6-well plates at a specific density.

To achieve 50 to 80% cell merging during transfection, perform cell seeding at 3×10^6 cells per well using 2mL of complete Dulbecco's Modified Eagle Medium (DMEM)/F12 media, which contains 2mM L-glutamine and 10% Fetal Bovine Serum (FBS). On the day of transfection, DNA-PEI complexes were prepared shortly before transfection by mixing 18.9 µg plasmid DNA diluted in 500µL serum-free DMEM with PEI at three different ratios (1:1, 1:2, and 1:3 DNA: PEI, w/w) to find the best transfection efficiency, as indicated by previous studies. The mixture was gently pipetted several times and left at room temperature for 15-20 minutes to allow the DNA-PEI polyplexes to form. The formed complexes were added dropwise to each well containing cells and 2mL of fresh complete DMEM/F12 medium, causing only a slight disturbance to the cell monolayer. Plates were gently rocked to evenly distribute the complexes and incubated at 37°C in a humidified 5% CO_2 atmosphere. After 18-20 hours, the medium was optionally replaced with fresh complete growth medium to minimise PEI-associated cytotoxicity and promote higher expression. Cells were subsequently maintained for an additional 24-48 hours to allow optimal protein expression before being harvested for downstream analyses. This is a generally adopted method for efficient stable transfection of mammalian cells and has been reported to give high levels of expression with minimal cytotoxicity when the proper DNA: PEI ratios are optimised[24].

2.5 Ni-NTA Affinity Purification of Recombinant Hyaluronidase

Recombinant hyaluronidase expressed in CHO-K1 cells was purified using Nickel-Nitrilotriacetic Acid (Ni-NTA) affinity chromatography. Culture supernatant was clarified by centrifugation and applied to a pre-equilibrated Ni–NTA column under normal conditions. The column was washed with buffer containing low imidazole to remove non-specific proteins. Bound His-tagged hyaluronidase was eluted using high-imidazole buffer, and fractions were collected for further analysis[25].

2.6 Animal Immunisation with Hyaluronidase (rHuPH20)

Rabbits were chosen as a sensitive species for producing antibodies against foreign proteins. Animal Ethical Approval Number -CPBL-IAEC-035/08/2023.

2.7 Production of IgG Antibodies Against Hyaluronidase

Rabbits (N=2) were selected for raising antibodies against hyaluronidase. Animals were immunised with 500µg of hyaluronidase with complete adjuvant at every 14-day interval. Followed by complete adjuvant, the animals were immunised with incomplete adjuvant at a dose of 250µg. Before each dose, the serum was collected from animals and titres were evaluated. Once a respectable (appropriate more than one lakh) titre was observed, the serum was collected from rabbits[26-28].

2.8 ELISA to Detect Antibody Titres

An indirect Enzyme-Linked Immunosorbent Assay (ELISA) method was used to evaluate the titers of the generated anti-hyaluronidase antibodies. Briefly, the Nunc plate was coated with 5µg/mL of hyaluronidase enzyme in carbonate-bicarbonate buffer (pH-9.5±0.5) and incubated overnight at 2-8°C. The following day, the plate was blocked using 2% Bovine Serum Albumin (BSA) in 1X Phosphate Buffered Saline with Tween (PBST) for an hour. Upon blocking unbound antigens, the plate was washed with 1X PBST for 3 times, and the samples were loaded in different dilutions in the blocked and washed plate for an hour. Followed by three washes with 1XPBST, a secondary Goat Anti-Rabbit IgG Horseradish Peroxidase (HRP) (1:8000) was loaded into the wells and incubated for an hour. After three washes with 1X PBST, the Tetramethylbenzidine (TMB) substrate was added to the wells, stopping the reaction using 1N H_2S0_4 [29-31]. The absorbance was measured at 450nm using a multimode microplate reader.

2.9 Bradford Protein Estimation

The Pierce™ Bradford Protein Assay Kit (Thermo Fisher Scientific, Catalogue No. 23200; 950 mL) was used for protein quantification.

2.10 Affinity Purification of Anti-Hyaluronidase IgG Antibodies

N-Hydroxysuccinimide (NHS) activated Sepharose column was used to purify the anti-hyaluronidase IgG antibodies. In brief, 3mg hyaluronidase enzyme was taken in coupling buffer (0.2M $NaHCO_3$, 0.5M NaCl, pH 8.3) with NHS-activated Sepharose beads (overnight incubation at 2-8°C in a rotator). The following day, coupled beads were blocked using 0.5M ethanolamine with 0.5M NaCl (pH 8.3 ± 0.3) for 3 hours. Wash the column with 12-15 bed volumes using high pH buffer, 0.1M Tris HCl with 0.5M NaCl with pH ranging from 8.0 to 9.0, followed by washing the column with low pH buffer, 0.1M acetate buffer with 0.5M NaCl (pH ranging from 4.0 to 5.0). At last, beads were stored in 0.1M Tris HCl with 0.5M NaCl.

For affinity purification of the anti-hyaluronidase antibody, the hyaluronidase-coated Sepharose beads were used. The beads were allowed to settle in the column, and the storage buffer was drained. Subsequently, the beads were washed 2-3 times with 1× PBS to remove residual buffer. Rabbit serum diluted 1:1 with PBS (5mL serum: 5mL PBS) was applied to the column and incubated on a rotator for 10-15 min to facilitate specific binding of anti-hyaluronidase antibodies to the immobilised hyaluronidase on beads.

Following incubation, the column was allowed to stand for bead settling. The column was then washed with 50mL of 1× PBS to remove unbound proteins and loosely associated impurities. Bound antibodies were eluted by passing approximately 5mL of 10 mM glycine buffer through the column twice, followed by rinsing with 1× PBS. The eluted fractions were dialysed for buffer exchange into PBS, aliquoted, and stored at −70 °C. This method was performed using the Cytiva kit (Catalog number-17090601)[32,33].

2.11 Affinity Purification of Hyaluronidase (rHuPH20) with Beads of Anti-hyaluronidase

Bead preparation was performed as described for the anti-hyaluronidase antibody in Section 2.9; however, cell culture medium was used instead of serum, as hyaluronidase was expressed and secreted into the medium.

2.12 Sodium Dodecyl Sulfate-Polyacrylamide Gel Electrophoresis (SDS-PAGE)

10% reducing gels were prepared, and samples (10µg) were loaded into the wells. Samples were denatured at 95°C for 5 mins. Upon denaturation, the samples were mixed with the loading dye and allowed to run at 80V. Upon completion of the run, the samples were stained using Coomassie brilliant blue staining, followed by destaining of the gel to check the purity of the purified antibodies[34,35].

2.13 Hyaluronidase Activity Assay

The enzymatic activity of hyaluronidase was obtained using a microplate-based turbidimetric assay. Each well contained 50µL of Hyaluronidase diluted in enzyme diluent (20mM sodium phosphate, 77mM sodium chloride, 0.01% BSA; pH 7.0 at 37°C). The mixtures were incubated at 37°C for 10 minutes. Following incubation, 100µL of potassium hyaluronic acid substrate solution (0.09% w/v in 300mM sodium phosphate buffer, pH 5.37 at 37°C) was added. The plate was mixed thoroughly and incubated at 37°C for 45 minutes.

The reaction was terminated and colour developed by transferring 40µL from each well into a flat-bottom plate preloaded with 200µL of acidic albumin solution (24mM sodium acetate, 79mM acetic acid, 0.1% BSA; pH 3.75 at 25°C). The plate was mixed and allowed to stand at room temperature for 10 minutes. Percentage transmittance (%T) was measured at 600nm using a multimode microplate reader. Enzyme activity was calculated relative to a standard curve generated with the Hyaluronidase Enzyme[36,37].

2.14 Data Analysis

Statistical analysis was done using GraphPad Prism 5.0 (Windows).

3. Results

A truncated variant of the recombinant human PH20 sequence was employed for cloning and expression, as the full-length wild-type sequence was non-permissive to secretion.

3.1 Structure Prediction

The predicted three-dimensional structure of recombinant human PH20 (rHuPH20) enzyme exhibited high confidence with an interface predicted TM (ipTM) score and pTM score both at 0.85, indicating reliable structural predictions suitable for MD simulations (Figure 1a).

3.2 Structural Stability Assessment

The total energy of the system stabilised at -211.997 kJ/mol, further confirming the thermodynamic stability of the structure. RMSD profiles of backbone atoms showed an initial equilibration phase within the first ~15ns, after which all systems converged to stable values with fluctuations of approximately ±0.05-0.1nm for the remainder of the 100ns simulation, indicating the absence of major conformational drift (Figure 1b).

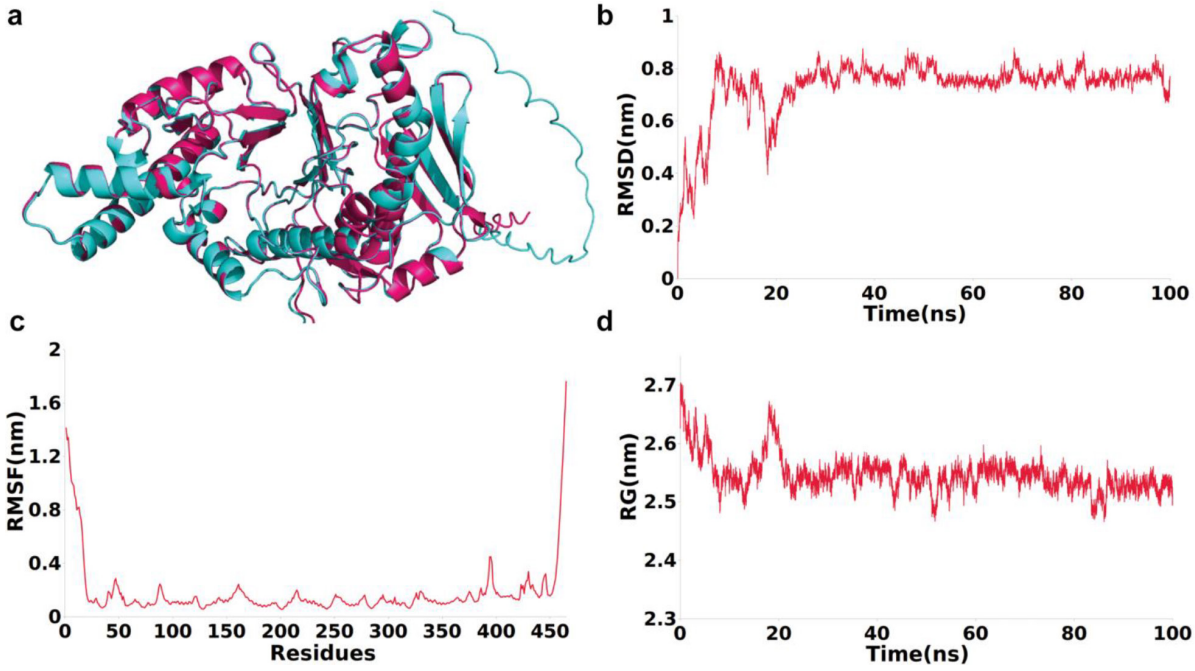


Figure 1. Structural stability of recombinant human hyaluronidase PH-20 (rHuPH20). **(a)** Superimposed three-dimensional structure of rHuPH20 (magenta) (Uniprot ID: P38567), **(b)** RMSD; **(c)** RMSF; **(d)** Radius of gyration as a function of time over 100 ns simulation.

RMSF analysis of Cα atoms revealed that residues comprising the structured core (α-helices and β-sheets) exhibited low flexibility, generally below 0.3-0.4nm, consistent with well-ordered secondary structural elements. Increased fluctuations were seen close to the C-terminal region, which most likely reflects the disordered terminal tails' intrinsic flexibility rather than the functional core's instability (Figure 1c). Rg profiles stabilised after initial equilibration and showed minimal variation around the mean, suggesting that the protein's overall compactness was maintained throughout the simulation (Figure 1d).

When combined, these metrics show that all systems reached stable conformations after equilibration and did not exhibit any significant structural drift over a period of 100ns. Among the variants examined, Variant 3 displayed the most consistent RMSD convergence, lowest residue-level fluctuations, and stable Rg profiles, suggesting it adopts a compact and well-ordered conformation under the simulated conditions.

3.3 Selection of Clones

In this study, a total of six recombinant clones were generated and subjected to a screening assay to identify the most promising candidate for downstream processing. In a microtiter ELISA plate, the supernatant was loaded at a 1:10 dilution. Clones were compared for the production of recombinant hyaluronidase. Among all the clones, on the basis of enzyme activity assay, E10 was found to be the best for further downstream processing.

3.4 Ni-NTA Affinity Purification of Recombinant Hyaluronidase

Hyaluronidase expressed in CHO-K1 cells was purified using nickel-nitrilotriacetic acid (Ni-NTA) affinity chromatography. The clarified culture supernatant was loaded onto a Ni–NTA column, allowing His-tagged hyaluronidase to bind, while unbound host proteins were removed during washing. The bound protein was eluted using imidazole. The purified hyaluronidase (~6mg from 40mL culture) was used for bead preparation and animal immunisation.

3.5 Titer Evaluation of Anti-Hyaluronidase IgG Antibodies

The immunogenicity of the recombinant hyaluronidase was assessed by ELISA, following the procedure described in the methods section. Serum collected from two immunised animals (N=2) was serially diluted and tested for antigen-specific IgG binding. The Optical Density (OD) values across the dilution series showed a clear and consistent antibody response against the enzyme.

The titers obtained correspond well with a previous study showing that hyaluronidase has the capability of creating a quantifiable immune response when given together with proper adjuvants. The titers obtained are consistent with a previous study demonstrating that, when administered in conjunction with appropriate adjuvants, hyaluronidase can elicit a measurable immune response.

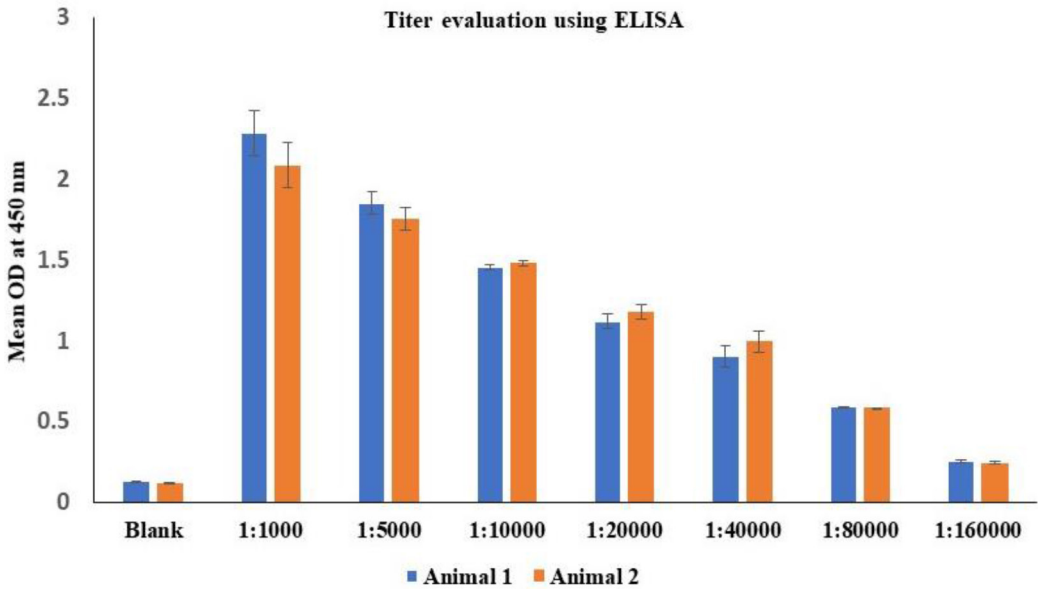


Figure 2. Graph shows the titer evaluation by ELISA.

These antibodies can be used for various purposes, such as hyaluronidase purification and analysis, as the calculated endpoint titer of 1:160,000 (Figure 2) indicates a very strong humoral response.

3.6 Anti-Hyaluronidase Antibody and rHuPH20 Assay

3.6.1 Bradford Assay results after affinity purification of anti-hyaluronidase antibody and rHuPH20

The estimated concentration of affinity-purified anti-hyaluronidase antibody was 1.1 mg/mL, and hyaluronidase (rHuPH20) was 1.2 mg/mL. Samples were aliquoted and stored at -70°C [38].

3.7 SDS-PAGE of Affinity-Purified Hyaluronidase

The purity of the Hyaluronidase was assessed using SDS-PAGE, as shown in Figure 3. The protein migrated as a clear band close to 55 kDa, which corresponds to the expected molecular size of hyaluronidase[38,39]. The presence of a single, very clear band with no additional bands makes it evident that the enzyme has been purified to an extremely high level through the purification steps. Thus, this level of purity is essential for the protein's subsequent experiments, such as determination of enzymatic activities, assessment of its immunogenicity, and continuation of structural studies.

3.8 The Enzyme Activity Assay of Hyaluronidase (rHuPH20)

The hyaluronidase enzyme activity assay was successfully performed, producing a clear and linear standard curve at 600nm across the tested concentration range. Hyaluronidase (rHuPH20) demonstrated measurable enzymatic activity. At a dilution factor of 5000, Hyaluronidase showed an activity of 109,656.41 IU/mL, while at 10,000 dilutions, the value was 108,199.90 IU/mL, as we can see in Figure 4B. These results indicate that rHuPH20 retains the best enzymatic activity. The standard curve generated from serial dilutions (100 to 0 IU/mL) exhibited strong linearity, with sample values

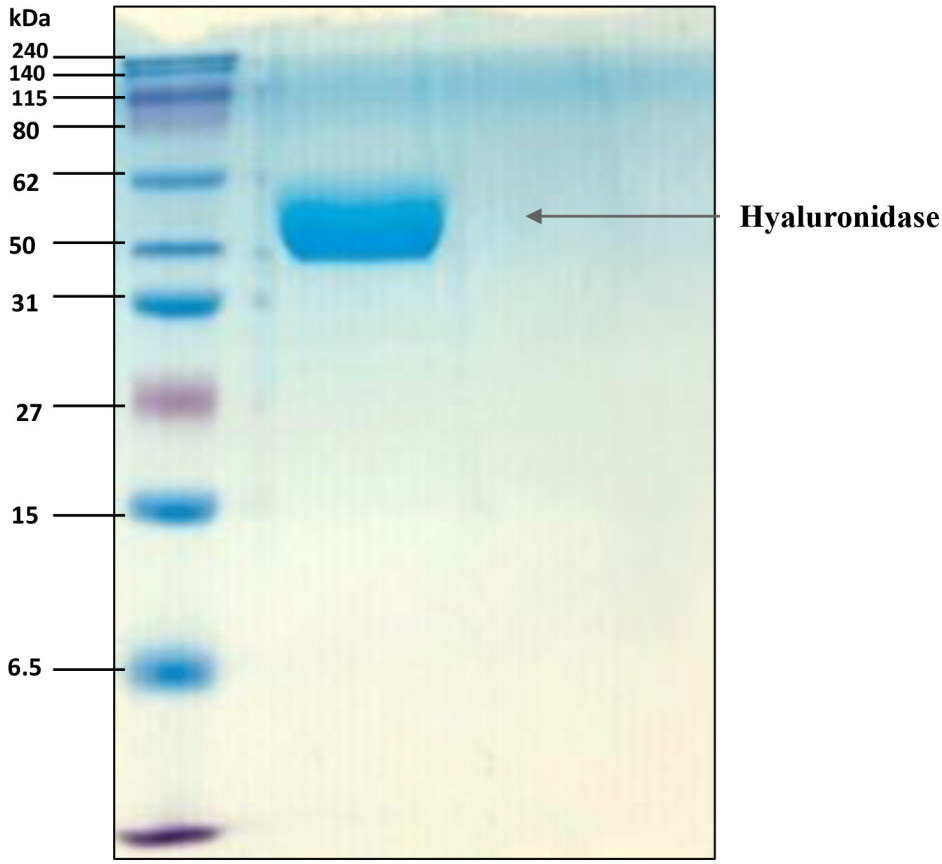
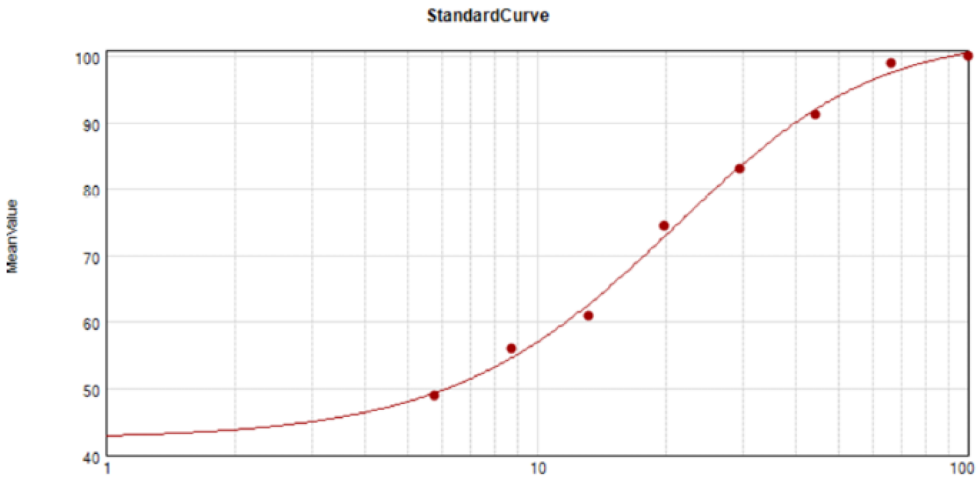


Figure 3. SDS -PAGE analysis of hyaluronidase.



Curve Fit : 5-Parameter Logistic $y = D + \frac{A - D}{\left\{1 + \left(\frac{x}{C}\right)^{B}\right\}^{G}}$

	Parameter	Estimated Value	Std. Error	Confidence Interval
Std R^2 = 0.997 EC50 = 19.59	A	42.48	1.579	[38.10, 46.86]
	B	1.600	0.383	[0.536, 2.664]
	C	26.72	27.57	[-49.83, 103.3]
	D	102.9	4.899	[89.31, 116.5]
	G	1.459	1.910	[-3.844, 6.761]

B

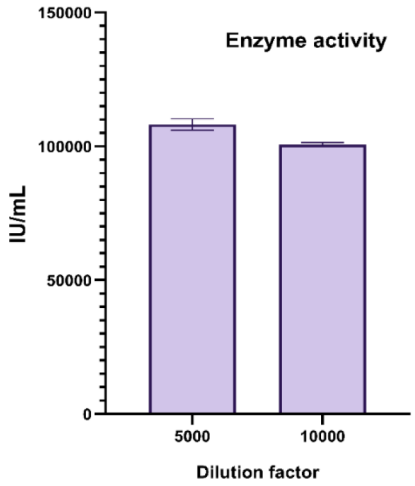


Figure 4. Enzyme activity assay for Hyaluronidase (rHuPH20): **(A)** Standard Curve; **(B)** Enzyme activity.

closely matching the expected concentrations (Figure 4A).

4. Discussion

The structural modelling and MD simulations of the recombinant human PH-20 (rHuPH20) hyaluronidase point to a very stable and reliable conformation. This is supported by high confidence scores from the structural prediction, specifically the ipTM and pTM confidence scores of 0.85. The thermodynamic profile of the system further confirmed that the folded state of the enzyme is energetically the most favourable, with the total energy stabilised at approximately 211.997 kJ/mol. RMSD analysis

reveals that the enzyme has stabilised and reached a state of equilibrium within the first 15ns and remains consistent throughout the 100 ns simulation. Previous studies report similar molecular dynamics behaviour for hyaluronidase and related enzymes, supporting the stability observed in this study. Both computational and experimental analyses show that hyaluronidase maintains a stable folded structure during simulations, with rapid equilibration and minimal structural deviation. Maksimenko and Sakharova, 2022, reported stable interaction dynamics with consistent energy profiles, while Guvench, 2022, showed that hyaluronan-processing enzymes retain structural integrity under physiological conditions[40,41].

RMSD analysis shows that proteins which reach equilibrium early in the simulation tend to remain stable over longer time periods. Similar observations were reported by Bharathi *et al.* 2016, where proteins retained their structural framework with only minor backbone changes. Feng *et al.*, 2025, also observed stable RMSD patterns along with compact structural behaviour in hyaluronidase systems[42,43]. In addition, stability is often supported by steady energy levels and consistent radius of gyration values. Kumar and Ojha, 2023, reported that stable enzymes usually display low energy variation and maintain compact structures during simulations. These earlier findings are in line with the present results. The engineered PH-20 hyaluronidase shows early RMSD stabilisation, stable energy behaviour, and compact folding, suggesting that the protein adopts a stable and energetically favourable conformation[44,45].

The RMSD values of backbone atoms (C, Cα, N) reached a plateau between 15 and 100ns, with very small fluctuations (±0.05nm). This indicates that the protein achieved a stable conformation after the initial relaxation phase and maintained this state for about 85ns. Since this plateau covers most of the simulation time, it supports true structural convergence rather than short-term stability. With RMSF analysis, we obtained detailed information about the flexibility of individual residues. There was very little movement in the catalytic and structural core region (residues 1-440), which is typical of an extremely rigid and well-folded domain. On the other side, the C-terminal tail past residue 450 shows quite a bit of motion, with RMSF values reaching around 1.6nm. Enhanced flexibility of this terminal piece could mean that it plays a role either in transient interactions or in the regulation of activities; nevertheless, this could also be simply a lack of structural restrictions in this particular region of the molecule. Moreover, the radius of gyration remained unchanged during the simulation, with only a slight decline from 2.65nm to 2.5nm, thus forming a tight, globular structure. The confirmation of the engineered PH-20 variant's integrity and native-like structure is suggested indirectly by this multi-parameter stability. Marković-Housley *et al.*, 2000, resolved the crystal structure of bee venom hyaluronidase and demonstrated that the enzyme maintains a conserved catalytic Triosephosphate Isomerase (TIM)-barrel-like core, while peripheral regions tolerate structural variation without disrupting global fold stability[46,47]. Similarly, Jedrzejas and Stern 2005, reported that bacterial hyaluronidases preserve catalytic architecture despite sequence diversity, indicating evolutionary robustness of the structural scaffold[48,49]. These Molecular dynamics simulations confirmed the stability of the rHuPH20 enzyme.

After transfection of the synthesised DNA, multiple clones were obtained, and on the basis of enzyme activity assay, the E10 clone was selected for its high productivity. Ata-Abadi *et al.*, 2022 showed that site-specific integration and clone selection improve PH20 yield, with ELISA confirming variation among clones[50,51]. Similarly, Liu *et al.*, 2016, reported variation in hyaluronidase expression among CHO-derived clones, emphasising the importance of systematic screening to identify high-producing candidates[52,53].

Recombinant Human Hyaluronidase (rHuPH20) was purified using a Ni-NTA affinity column, yielding approximately 6mg of protein. The purified protein was used for rabbit immunisation to generate anti-hyaluronidase antibodies and was also applied in bead preparation.

Following immunisation with Ni-NTA-purified rHuPH20, the rabbit showed a strong immune response, producing a high level of anti-hyaluronidase antibodies, with titers reaching approximately 1:160,000 as determined by indirect ELISA. The antibodies were further purified using hyaluronidase-conjugated beads. This affinity-purified polyclonal antibody was then coupled to NHS beads and used for hyaluronidase purification, resulting in a higher level of purity compared to the initial Ni-NTA step.

To confirm expression and purification, SDS-PAGE analysis was performed. A distinct single band at approximately 55 kDa was observed, indicating high purity and absence of aggregation, and confirming the effectiveness of the affinity purification process. Enzyme

activity was evaluated at two dilutions (5,000 and 10,000), and both showed comparable activity levels of approximately 100,000 units. These results indicate that the purified enzyme retains high functional activity.

5. Conclusion

The three-dimensional structure of recombinant human PH-20 (rHuPH20) appears stable and compact, as supported by consistent molecular dynamics simulation parameters and favourable thermodynamic behaviour. Low RMSD and RMSF values within the catalytic core, together with a stable radius of gyration, indicate that the enzyme preserves its structural integrity under physiological conditions. Among the screened clones, E10 was identified as the most efficient producer. The purified enzyme showed a single prominent band at approximately 55 kDa on SDS-PAGE, confirming successful expression and a high level of purity. A strong IgG response was observed after three rounds of immunisation, with endpoint titers of approximately 1:160,000, suggesting that the recombinant human protein is immunogenic in rabbits and suitable for antibody production. Overall, these results suggest that recombinant human PH20 is structurally stable and can be efficiently expressed. However, additional studies, including detailed enzymatic kinetics, substrate specificity, and stability under different conditions, are required to further define its biotechnological applications and potential therapeutic use.

6. Acknowledgements

The Authors are highly obliged for the kind and needful support of the Department of Biotechnology (DBT)-funded Bioinformatics Centre and the "Workshop in Bioinformatics" project, along with the Department of Science and Technology- Fund for Improvement of Science and Technology (DST-FIST) program under Banasthali Vidyapith, for providing the necessary facility to conduct this study. The authors also express their deepest gratitude to Prof. Ina Shastri, Vice Chancellor, Banasthali Vidyapith, for her support.

7. References

1. Weber GC, Buhren BA, Schrumpf H, Wohlrab J, Gerber PA. Clinical applications of hyaluronidase. In: Therapeutic enzymes: Function and clinical implications. 2019. p. 255-277. https://doi.org/10.1007/978-981-13-7709-9_12 PMid:31482503.
2. Garantziotis S, Savani RC. Hyaluronan biology: A complex balancing act of structure, function, location and context. Matrix Biol. 2019; 78:1-10. https://doi.org/10.1016/j.matbio.2019.02.002 PMid:30802498 PMCid:PMC6774756.
3. Passi A, Vigetti D. Hyaluronan: Structure, metabolism, and biological properties. In: Cohen, E., Merzendorfer, H. (eds) Extracellular Sugar-Based Biopolymers Matrices. . Biologically-Inspired Systems, Cham. p. 155-186. https://doi.org/10.1007/978-3-030-12919-4_4 https://doi.org/10.1007/978-3-030-12919-4_4
4. Meyer K. Hyaluronidases. In: The enzymes. Academic Press. 1971; 5:307-320. https://doi.org/10.1016/S1874-6047(08)60094-3
5. Nonoguchi HA, Liu GY, Hajam IA. Microbial hyaluronidases: From obscure virulence factors to promising therapeutic targets. Biomolecules. 2026; 16(4):516. https://doi.org/10.3390/biom16040516 PMid:42072637 PMCid:PMC13113925.
6. Grinkova AA, Ustyuzhanina NE, Nifantiev NE. Synthesis of oligosaccharides structurally related to hyaluronic acid fragments. Russ J Bioorg Chem. 2022; 48(2):191-220. https://doi.org/10.1134/S1068162022020108
7. Ibraheem MA, Elfakharany EM, Moussa S, Mohammed FAR. An overview on hyaluronidase enzyme types, mode of action, assay and therapeutic applications. J Sci Res Sci. 2024; 41(2):1-17. https://doi.org/10.21608/jsrs.2024.273369.1125
8. Zhang L, Bharadwaj AG, Casper A, Barkley J, Barycki JJ, Simpson MA. Hyaluronidase activity of human Hyal1. J Biol Chem. 2009; 284(14):9433-9442. https://doi.org/10.1074/jbc.M900210200 PMid:19201751 PMCid:PMC2666596.
9. Wang W, Wang J, Li F. Hyaluronidase and chondroitinase. Protein Rev. 2016; 17:75-87. https://doi.org/10.1007/5584_2016_54 PMid:27677277.
10. Zhang L, Bharadwaj AG, Casper A, Barkley J, Barycki JJ, Simpson MA. Hyaluronidase activity of human Hyal1 requires active site acidic and tyrosine residues. J Biol Chem. 2009; 284(14):9433-9442. https://doi.org/10.1074/jbc.M900210200 PMid:19201751 PMCid:PMC2666596.
11. Feng QP, Zhu YT, Yuan YZ, Li WJ, Yu HH, Hu MY, Yu SQ. Oral administration co-delivery nanoparticles of docetaxel and bevacizumab for improving intestinal absorption and enhancing anticancer activity. Mater Sci Eng C. 2021; 124:112039. https://doi.org/10.1016/j.msec.2021.112039 PMid:33947539.
12. Badkar AV, Gandhi RB, Davis SP, Labarre MJ. Subcutaneous delivery of high-dose/volume biologics: Current status and prospect for future advancements. Drug Des Devel Ther. 2021; 15:159-170. https://doi.org/10.2147/DDDT.S287323 PMid:33469268 PMCid:PMC7812053.

13. Guo J, Weng J, Zhou F, Gu X. An industry perspective on hyaluronidase coformulated bi1opharmaceutics. J Control Release. 2025; 381:113573. https://doi.org/10.1016/j.jconrel.2025.02.069 PMid:40010413.
14. Knowles SP, Printz MA, Kang DW, LaBarre MJ, Tannenbaum RP. Safety of recombinant human hyaluronidase PH20 for subcutaneous drug delivery. Expert Opin Drug Deliv. 2021; 18(11):16731685. https://doi.org/10.1080/17425247.2021.1981286 PMid:34585991.
15. Meglio M. Subcutaneous infusion of ocrelizumab using ENHANZE technology shows noninferiority to intravenous formulation. Neurology Live. 2023.
16. Ziegengeist JL, Tan AR. A clinical review of subcutaneous trastuzumab and the fixeddose combination of pertuzumab and trastuzumab for subcutaneous injection in the treatment of HER2positive breast cancer. Clin Breast Cancer. 2025; 25(2):e124e132. https://doi.org/10.1016/j.clbc.2024.10.005 PMid:39567339.
17. Kang DW, Connor RJ, Nekoroski T, Bitsura JAM, Kindig SK, Knowles SP, LaBarre MJ. A phase I clinical study to evaluate rapid, high-volume, subcutaneous auto-injector tolerability with recombinant human hyaluronidase. Drug Deliv Transl Res. 2025; 1-13. https://doi.org/10.1007/s13346-025-01883-z PMid:40445528 PMCid: PMC12682915.
18. Desai M, Kundu A, Hageman M, Lou H, Boisvert D. Monoclonal antibody and protein therapeutic formulations for subcutaneous delivery: high-concentration, low-volume vs. low-concentration, high-volume. MAbs. 2023; 15(1):2285277. https://doi.org/10.1080/19420862.2023.2285277 PMid:38013454 PMCid:PMC10793682.
19. van Karnebeek CDM, Wortmann SB, Tarailo-Graovac M, Langeveld M, Ferreira CR, van de Kamp JM, *et al.* The role of the clinician in the multi-omics era: Are you ready? J Inherit Metab Dis. 2018; 41:437-446. https://doi.org/10.1007/s10545-017-0128-1 PMid:29362952 PMCid:PMC5959952.
20. Yeh HJ, Lai JR, Cheng TC. Advancing subcutaneous delivery of biologics: A novel reusable MEMS-enabled actuator. Drug Deliv Transl Res. 2024; 14(2):117-126.
21. Park C, Song YK, Kim YH, Jung Y, Park YH, Song BS, Kim E. Development of a new type of recombinant hyaluronidase using a hexahistidine; Possibilities and challenges in commercialization. J Microbiol Biotechnol. 2019; 29(8):1310-1315. https://doi.org/10.4014/jmb.1905.05049 PMid:31370115.
22. Park SJ, Kim K, Yun SH, Cho JS, Park K, Byun M, Nam KS. U.S. Patent No. 12,221,638. Washington, DC: U.S. Patent and Trademark Office; 2025.
23. Jumper J, Evans R, Pritzel A, Green T, Figurnov M, Ronneberger O, *et al.* AlphaFold structure prediction. Nature. 2021; 596:583-589. https://doi.org/10.1038/s41586-021-03819-2 PMid:34265844 PMCid:PMC8371605.
24. Abraham MJ, Murtola T, Schulz R, Páll S, Smith JC, Hess B, *et al.* GROMACS: High-performance molecular simulations through multi-level parallelism from laptops to supercomputers. SoftwareX. 2015; 1-2:19-25. https://doi.org/10.1016/j.softx.2015.06.001
25. Huang J, MacKerell AD. CHARMM36 all-atom additive protein force field. J Comput Chem. 2013; 34(25):2135-2145. https://doi.org/10.1002/jcc.23354 PMid:23832629 PMCid:PMC3800559.
26. Boussif O, Lezoualc'h F, Zanta MA, Mergny MD, Scherman D, Demeneix B, *et al.* A versatile vector for gene and oligonucleotide transfer into cells: Polyethylenimine. Proc Natl Acad Sci U S A. 1995; 92(16):7297-7301. https://doi.org/10.1073/pnas.92.16.7297 PMid:7638184 PMCid:PMC41326.
27. Longo PA, Kavran JM, Kim MS, Leahy DJ. Transient mammalian cell transfection with PEI. Methods Enzymol. 2013; 529:227-240. https://doi.org/10.1016/B978-0-12-418687-3.00018-5 PMid:24011049 PMCid:PMC4012321.
28. Durocher Y, Perret S, Kamen A. High-level recombinant protein production by transient transfection. Nucleic Acids Res. 2002; 30(2):e9. https://doi.org/10.1093/nar/30.2.e9 PMid:11788735 PMCid:PMC99848.
29. Spriestersbach A, Kubicek J, Schäfer F, Block H, Maertens B. Purification of his-tagged proteins. In Methods Enzymol. 2015; 559:1-15. Academic Press. https://doi.org/10.1016/bs.mie.2014.11.003 PMid:26096499.
30. Leenaars M, Hendriksen CFM. Critical steps in antibody production. ILAR J. 2005; 46(3):269. https://doi.org/10.1093/ilar.46.3.269 PMid:15953834.
31. Horta CCR, Magalhães BD, Oliveira-Mendes BB, Carmo AO, Duarte CG, Felicori LF, *et al.* Molecular, Immunological, and Biological Characterization of *Tityus serrulatus* venom hyaluronidase: new insights into its role in envenomation PLoS Negl Trop Dis. 2014; 8(2):e2693. https://doi.org/10.1371/journal.pntd.0002693
32. Cooper HM, Patterson Y. Production of polyclonal antisera. Curr Protoc Immunol. 2008; 82(1):2.4.1-2.4.10. https://doi.org/10.1002/0471142735.im0204s82 PMid:18729062.
33. Halperin SA, Gray ED, Ferrieri P, Wannamaker LW. ELISA for antibodies to group A streptococcal bacteriophage. J Lab Clin Med. 1985; 106(5):505-511. https://doi.org/10.1128/iai.27.1.118-123.1980 PMid:6987164 PMCid: PMC550733.
34. Lin AV. (2015). Indirect elisa. In ELISA: methods and protocols (pp. 51-59). New York, NY: Springer 2015. p. 51-9.
35. Cliquet F, McElhinney LM, Servat A, Boucher JM, Lowings JP, Goddard T, et al. 2004). Development of a qualitative indirect ELISA for the measurement of rabies virus-specific antibodies from vaccinated dogs and cats. J Virol Methods. 2004; 117(1):1-8.
36. Wofsy L, Burr B. The use of affinity chromatography for the specific purification of antibodies and antigens. J

Immunol. 1969; 103(2):380-382. https://doi.org/10.4049/jimmunol.103.2.380 PMid:4184826.
37. Grodzki AC, Berenstein E. Antibody purification: Affinity chromatography-protein A and protein G Sepharose. In: Immunocytochemical methods and protocols. Totowa (NJ): Humana Press; 2009; p. 33-41. https://doi.org/10.1007/978-1-59745-324-0_5 PMid:20012816.
38. Bradford MM. A rapid and sensitive method for the quantitation of microgram quantities of protein. Anal Biochem. 1976; 72:248-254. https://doi.org/10.1016/0003-2697(76)90527-3 PMid:942051.
39. Harlow E, Lane D. Antibodies: A laboratory manual. Cold Spring Harbor, NY: Cold Spring Harbor Laboratory Press; 1988.
40. Bordon KC, Santos GC, Martins JG, Wiezel GA, Amorim FG, Crasset T, Arantes EC. Pioneering comparative proteomic and enzymatic profiling of Amazonian scorpion venoms enables the isolation of their first α-Ktx, metalloprotease, and phospholipase A2. Toxins. 2025; 17(8):411. https://doi.org/10.3390/toxins17080411 PMid:40864087 PMCid: PMC12390242.
41. Olgen S, Kaeßler A, Nebioğlu D, Jose J. New potent indole derivatives as hyaluronidase inhibitors. Chem Biol Drug Des. 2007; 70(6):547-551. https://doi.org/10.1111/j.1747-0285.2007.00590.x PMid:17986205.
42. Modarressi SM, Akbari M. Enhancing hyaluronidase enzyme activity. J Chromatogr B. 2024; 1234:124031. https://doi.org/10.1016/j.jchromb.2024.124031 PMid:38330521.
43. Afify AM, Stern M, Guntenhöner M, Stern R. Purification and characterization of human serum hyaluronidase. Arch Biochem Biophys. 1993; 305(2):434-441. https://doi.org/10.1006/abbi.1993.1437.
44. Maksimenko AV, Sakharova YS, Beabealashvilli RS. Experimental and computational study of hyaluronidase interactions with glycosaminoglycans and their ligands. Curr Mol Med. 2022; 22(8):675-690. https://doi.org/10.2174/1566524021666211018113204 PMid:35708105.
45. Guvench O. Atomic-resolution experimental structural biology and molecular dynamics simulations of hyaluronan and its complexes. Molecules. 2022; 27(21):7276. https://doi.org/10.3390/molecules27217276 PMid:36364098 PMCid:PMC9658939.
46. Bharathi AC, Yadav PK, Syed Ibrahim B. Sequence diversity and ligand-induced structural rearrangements of viper hyaluronidase. Mol Biosyst. 2016; 12(4):1128-1138. https://doi.org/10.1039/C5MB00786K PMid:26867694.
47. Marković-Housley Z, Miglierini G, Soldatova L, Rizkallah PJ, Müller U, Schirmer T. Crystal structure of hyaluronidase, a major allergen of bee venom. Structure. 2000; 8(10):1025-1035. https://doi.org/10.1016/S0969-2126(00)00511-6 PMid:11080624.
48. Feng Z, Li J, Li SJ. Molecular insight into the inhibitory effect of sulfated polysaccharide fucoidan on hyaluronidase activity. J Agric Food Chem. 2025; 73(34):21621-21630. https://doi.org/10.1021/acs.jafc.5c04257 PMid:40825373.
49. Jedrzejas MJ, Stern R. Structures of vertebrate hyaluronidases and their unique enzymatic mechanism of hydrolysis. Proteins. 2005; 61(2):227-238. https://doi.org/10.1002/prot.20592 PMid:16104017.
50. Kumar A, Ojha KK. Molecular dynamics simulation methods to study structural dynamics of proteins. In: Protein folding dynamics and stability: Experimental and computational methods. Singapore: Springer Nature Singapore. 2023; p. 83-106. https://doi.org/10.1007/978-981-99-2079-2_5.
51. Ata-Abadi NS, Forouzanfar M, Dormiani K, Varnosfaderani SR, Pirjamali L, Nasr-Esfahani MH, Hajidavaloo RM. Site-specific integration as an efficient method for production of recombinant human hyaluronidase PH20 in semi-adherent cells. Appl Microbiol Biotechnol. 2022; 106(4):1459-1473. https://doi.org/10.1007/s00253-022-11794-5 PMid:35107633.
52. Pande V, Joshi T, Pandey SC, Sati D, Mathpal S, Pande V, Samant M. Molecular docking and molecular dynamics simulation approaches for evaluation of laccase-mediated biodegradation of various industrial dyes. J Biomol Struct Dyn. 2022; 40(23):12461-12471. https://doi.org/10.1080/07391102.2021.1971564 PMid:34459700.
53. Liu S, Xie B, Wei W, Hui M, Su Z. Design and preparation of chimeric hyaluronidase as a chaperone for the subcutaneous administration of biopharmaceuticals. Biochem Eng J. 2016; 112:32-41. https://doi.org/10.1016/j.bej.2016.03.013

Author Contributions

Conceptualisation-R.B. and A.P.; Methodology- C.G.P., E.T and A.K.; Investigation-C.G.P., E.T., A.K., and PJ.; Writing-Original Draft-C.G.P., E.T. and A.K.; Writing-Review& Editing- R.B. and A.P. All authors read and approved the final manuscript.

Access this journal online	
Website: https://informaticsjournals.com/journals/toxi/home	**Quick Response Code**